Renewable and Sustainable Energy Reviews 16 (2012) 6678–6685

Contents lists available at SciVerse ScienceDirect

Renewable and Sustainable Energy Reviews

journal homepage: www.elsevier.com/locate/rser

Power, placement and LEC evaluation to install CSP plants in northern Chile

Nicolás Corral, Nicolás Anrique *, Dalila Fernandes, Cristóbal Parrado, Gustavo Cáceres

Facultad de Ingeniería y Ciencias, Universidad Adolfo Ibáñez, Diagonal Las Torres 2640, Peñalolén, Santiago, Chile

ARTICLE INFO

Article history:
Received 12 May 2012
Accepted 5 September 2012
Available online 5 October 2012

Keywords:
CSP plant
Solar radiation
Northern Chile
LEC
Power plant capacity
Back-up and TES system
Placement evaluation

ABSTRACT

Chile is expecting a 5.4% growth in energy consumption per year until 2030, requiring new and better solutions for the upward trend of its electricity demand. This state leads to select and study one of the potential alternatives for electricity generation: concentrated solar power (CSP) plants. Such renewable technology found in Chile a very favorable condition. Recent researches indicate Atacama Desert as one of the best regions for solar energy worldwide, having an average radiation higher than in places where CSP plants are currently implemented, e.g. Spain and USA. The aim of this study is to present an analysis of levelized energy cost (LEC) for different power capacities of CSP plants placed in distinct locations in northern Chile. The results showed that CSP plants can be implemented in Atacama Desert with LECs around 19 ¢US$/kWh when a gas-fired backup and thermal energy storage (TES) systems are fitted. This value increases to approximately 28 ¢US$/kWh if there is no backup system.

Contents

1. Introduction

Chile is nowadays passing through a period of uncertainty in what regards its energy sector, which is found to be unprepared to provide the estimated growth of 5.4% in energy consumption per year until 2030 [1]. The current energy situation in Chile and its radiation conditions gives the opportunity to investigate the potential and viability of implementing solar thermal power plants in the north of the country [2–4]. However, there are only few researches available in this subject regarding Chile, and the majority of them date from two or three decades ago [5–9]. In addition to that, it is noted that none of the existing researches consider economic aspects to install a concentrated solar plant in Chile.

Regarding Chilean energy regulations, it is important to remark that, since 2008, the electricity companies selling directly to final customers must incorporate a certain percentage of non-conventional renewable energy (NCRE) into the electricity they trade [10]. This law consolidates the efforts to remove barriers to the incorporation of NCRE into the national power mix, thereby

Abbreviations: CSP, concentrated solar power; LEC, levelized energy cost; SPT, solar parabolic trough; TES, thermal energy storage; NCRE, non-conventional renewable energy; SIC, electric central interconnected system; SING, electric northern interconnected system; UTFSM, Universidad Técnica Federico Santa María; NSA, national solarimetric archive; DNI, direct normal irradiance; HTF, heat transfer fluid; PB, power block; PTC, parabolic trough collector; DSG, direct steam generation; AIC, annual electricity generation; TICVC, total investment costs and variable costs

* Corresponding author. Tel.: +56 2 4747246.
E-mail address: n.anrique@ieee.org (N. Anrique).

1364-0321/$ - see front matter © 2012 Elsevier Ltd. All rights reserved.
http://dx.doi.org/10.1016/j.rser.2012.09.006

contributes to the objectives of supply security and environmental sustainability that govern Chile's energy policy. Nevertheless, according to the latest official report on the subject [10], the supply of energy in Chile is primarily provided by conventional power plants, as coal-fired thermal plants, combined cycle, diesel engines, gas/oil turbines, and large scale hydro electrical power plants. As shown in Fig. 1, in 2010, only approximately 3% of the energy was produced by non-conventional renewable power plants (small hydro, biomass, and wind). In the same year, from a total of 14.878 MW of installed capacity (Fig. 2), only 3.1% was NCRE plants.

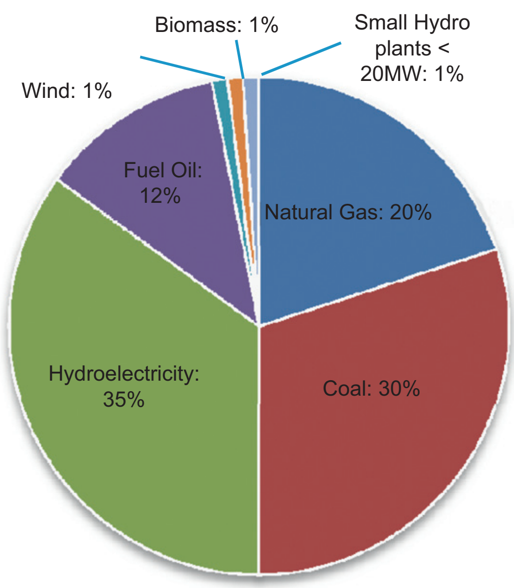


Fig. 1. Electricity generation in Chile (SIC and SING) during 2010 [10].

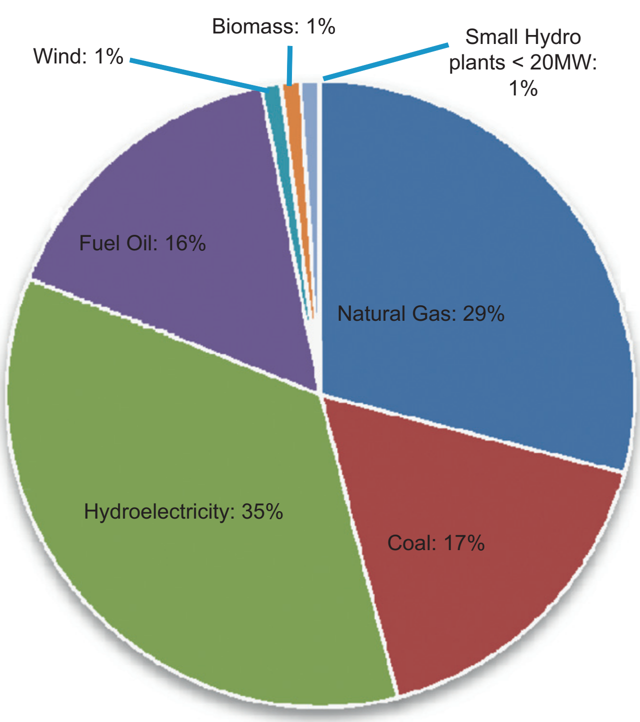


Fig. 2. Installed capacity in Chile (SIC and SING) by generation technology in 2010 [10].

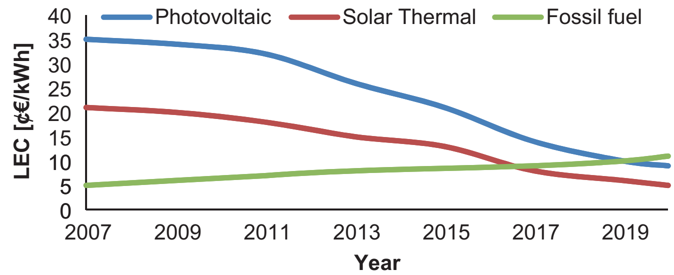


Fig. 3. Forecast of LEC values for different generation technologies [14,13].

The statistics show that there is a very favorable scenario for absorbing new NCRE projects needed to accomplish the percentage of NCRE officially required. Therefore, in order to encourage private and public investments in solar thermal energy, it is necessary for the national academic community to provide novel studies and tools in which technical and economic analysis can rely on. Concentrated solar power (CSP) technology has been widely investigated and enhanced in many countries [11,12], and these studies serve as a solid basis for newer investigations of CSP technology applied to the Chilean context. Moreover, it has been found that, for the next few years, costs of solar thermal energy generation present a trend of decrease, while the fossil-fuel alternative presents an upward evolution. According to Fig. 3 [13–15], it is possible for solar thermal energy costs to be at the same level of fossil-fuel energy costs around 2020.

Considering all explained above, the present study aims to develop an economic analysis for computing the LEC acquired from different CSP plant sizes in distinct locations in northern Chile. The research basis lay on contributions of recent Chilean researches [2,4] together with international researches [16–21] in order to evaluate the implementation of CSP plants in the north of the country. The analysis is undertaken through a computational simulation, which is performed for two different plant arrangements: the first consists in a solar parabolic trough (SPT) power plant fitted with thermal energy storage (TES) system and a gas-fired backup system; and a second configuration of a SPT plant equipped only with a TES system. Thereby, the simulation allows determining the plant power capacity and configuration that provides the lowest LEC among the different locations selected.

2. Potential for concentrated solar plants in northern Chile

Recent researches regarding the potential of solar radiation in northern Chile [2,4]indicates the Atacama Desert as being one of the best worldwide regions for solar energy, based on energy density data from several sources [22–25]. According to them, the region presents a high number of clear days during the year, due to the aridity of the Atacama Desert, defined as a hyperacid region [26] with annual average precipitations lower than 50 mm per year. This research considered the solar radiation data presented by [27] also available at [24], which is derived from ground station measurements compiled by Universidad Técnica Federico Santa María (UTFSM). More discussion about the solar energy data in Chile and its uncertainty levels can be found in the literature [25]. Table 1 [4,18] and Fig. 4 [27] show that the average radiation in the north of Chile is even higher than in some places where solar power plants are currently implemented.

For the economic evaluation of CSP plants, the present study accounts not only the Atacama Desert but also the several locations in northern Chile within the SING (northern electric interconnected system) area. It is considered that different

regions in this territorial range have a strong potential for placing CSP plants.

In the following section, the solar radiation data extracted from monthly means provided by UTFSM is processed in order to create an hourly database. The location and technology selection are also presented, as well as the method used for calculating the final energy produced from the available solar radiation. Finally, an analysis of the Levelized Energy Costs (LEC) is proposed for establishing the most suitable plant size and configuration required for each region analyzed.

3. Methodology

3.1. Estimation of available solar radiation and location selection

About 16 locations in the Atacama Desert are presented in the UTFSM data and chosen for evaluation, all of them situated between -18.20° y -26.27° latitudes and -70.46° y -68.01° longitudes.

In the country, four radiation databases are available to the public, all of them obtained by different ground station networks:

- National Solarimetric Archive (NSA): 89 stations.
- Meteorological service data: 18 stations.
- CNE-GTZ ground stations: 7 stations.
- UC-FONDEF ground stations: 12 stations.

The radiation data used for the simulations were acquired from the national solarimetric archive [27], which include data covering from 1961 to 1983. In comparison with the additional databases, NSA registrations are in between the others, with moderately low radiation levels, making it appropriate for economic evaluations in a worst-case scenario.

In the locations selected, solar radiation peaks during summertime at values close to 900 MJ/m^2 month, with winter minima nearing 260 MJ/m2 month. Fig. 4 shows global average irradiance per month per square meter.

Table 1
Solar radiation of CSP plants and projects [4,18].

Plant	Location	Radiation kWh/m^2 day
Plataforma Solar Almeria	Almeria, Spain	4.82
SEGS	California, USA	5.86
Abengoa ISCCS project	Ain-Ben-Mathar, Moroco	4.84
Not developed yet	North Chile	≈ 6

Chilean solar radiation data are available only in the form of monthly means measurements of the daily total radiation (H □ for each location).Therefore, it is necessary to apply a methodology that converts these values into hourly databases, a more accurate data to use as an input in the power plant simulation. Considering that a CSP plant will only accept direct normal irradiance (DNI) in order to work, the main objective is to develop a model for calculating the clear days. The procedure used is outlined by Duffie and Beckman [23], and is based on the Liu and Jordan [28] generalized distributions of cloudy and clear days, later modified by Bendt et al. [29,30], then by Stuarts and Hollands [31] and finally by Knight [32]. Based on this theoretical background, the hourly radiation beam is obtained using a correlation method described in [4,23,32,33]: first, an artificial daily total radiation H is obtained for each day of the month; then, an artificial month of daily and hourly values of solar radiation is built; finally, the clear day model is applied to obtain hourly values.

3.2. Estimation of daily radiation

For converting available data into hourly database, the previously mentioned methodology is based in the clearness index (K_T), which is the ratio between daily radiation in a horizontal surface and the extraterrestrial radiation. The selected procedure is also used in [4] and is described essentially in [23].

First, it is necessary to compute monthly average clearness index ($\overline{K}_T$) for each month and location, which is defined as

$$\overline{K}_T = \frac{\overline{H}}{\overline{H}_0} \tag{1}$$

where $\overline{H}$ is the monthly average radiation, obtained from the registered measurements in [27], and $\overline{H}_0$ is the monthly average extraterrestrial radiation, computed for each day and location by the following formula:

$$H_0 = \frac{24 \times 3600 \times G_{SC}}{\pi}\left(1+0.033\cos\frac{360n}{365}\right)(\cos(\phi)\cos(\delta)\sin(w_s) + w_s\sin(\phi)\sin(\delta)) \tag{2}$$

Here, G_{SC} is the solar constant, which is the energy of the sun per unit time, received on a unit area of a surface perpendicular to the propagation direction of the radiation, at mean earth–sun

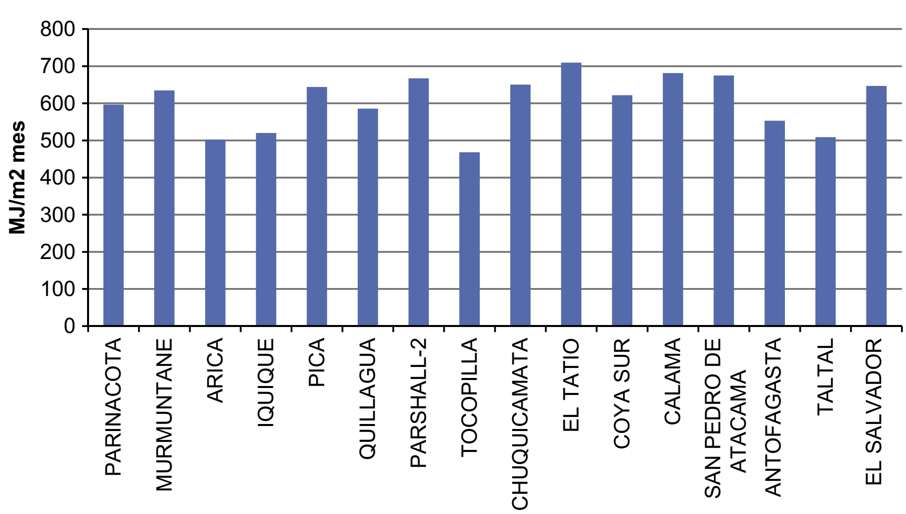


Fig. 4. Average monthly global irradiance in locations selected [27].

distance, outside of the atmosphere. A value for G_{SC} of 1367 $[W/m^2]$ is used in this paper. Also n is the n-day of the year, ϕ is the latitude in radians, δ is the declination angle in radians, and w_s is the sunset hour angle in radians. The declination angle is defined by the equation of Cooper [34] as

$$\delta = 23.45 \sin\left(360\left(\frac{284+n}{365}\right)\right) \tag{3}$$

And the sunset hour angle, when the incidence angle is 90°, as is needed for CSP plants [29], is defined as

$$\cos(w_s) = -\tan(\phi)\tan(\delta) \tag{4}$$

Then, it's assigned a special distribution to the frequency of days with a value of the clearness index K_T. The fraction f of the days in the month that are less clear than K_T is defined with the Bendt correlation as function of $\overline{K}_T$ [29]

$$f(K_T) = \frac{e^{(\gamma K_{T,\min})} - e^{(\gamma K_T)}}{e^{(\gamma K_{T,\min})} - e^{(\gamma K_{T,\max})}} \tag{5}$$

where γ is a dimensionless parameter given by

$$\gamma = -1.498 + \frac{1.184\xi - 27.182 \cdot e^{(-1.5\xi)}}{K_{T,\max} - K_{T,\min}} \tag{6}$$

where ξ is also a dimensionless parameter given by

$$\xi = \frac{K_{T,\max} - K_{T,\min}}{K_{T,\max} - \overline{K}_T} \tag{7}$$

The minimum and maximum values of K_T, $K_{T,min}$, and $K_{T,max}$, respectively, are given by

$$K_{T,\max} = 0.6313 + 0.267\overline{K}_T - 11.9(\overline{K}_T - 0.75)^8 \tag{8}$$

$$K_{T,\min} = 0.05 \tag{9}$$

To obtain a daily clearness index, Knight [9] defines daily K_T as

$$K_T = \frac{\ln\left[\left(1 - \frac{nd_k - 1/2}{ndm}\right) e^{(\gamma K_{T,\min})} + \left(\frac{nd_k - 1/2}{ndm}\right) e^{(\gamma K_{T,\max})}\right]}{\gamma} \tag{10}$$

where nd_k is the day of the month and ndm is the number of days of the month.

With all mentioned equations solved, artificial months with artificial daily radiations (H) are created, where months are arranged from lowest to highest H. Although this procedure neglects the autoregressive nature of solar radiation, according to Larraín et al. [4], it can be used as a first approximation that, nevertheless, constitutes an improvement from monthly mean computations.

3.3. Estimation of hourly diffuse and beam radiation

As CSP plants accept only DNI, diffuse radiation is subtracted from global radiation to obtain the beam radiation, which is the one we are interested. The daily diffuse radiation (H_d) is defined by Erbs correlations in [29], where depending on the sunset hour angle (w_s), the daily total diffuse fraction is defined as

For $w_s \le 81.4^\circ$

$$\frac{H_d}{H} = \begin{cases} 1 - 0.2727K_T + 2.4495{K_T}^2 - 11.951{K_T}^3 \\ \quad + 9.3879{K_T}^4, \quad K_T < 0.715 \\ \quad 0.143, \quad K_T \ge 0.715 \end{cases} \tag{11}$$

And for $w_s > 81.4^\circ$

$$\frac{H_d}{H} = \begin{cases} 1 + 0.2832K_T - 2.5557{K_T}^2 \\ + 0.8448{K_T}^3, \quad K_T < 0.715 \\ \quad 0.175, \quad K_T \ge 0.715 \end{cases} \tag{12}$$

With H and H_d calculated for each day, hourly radiation (I) is obtained by the ratio of hourly to daily total radiation (r_t),which is defined as the following equation from Collares–Pereira and Rabl [29] as function of the hour angle (w in radians) and the sunset hour angle (w_s):

$$r_t = \frac{I}{H} = \frac{\pi}{24}(a + b\cos(w))\left(\frac{\cos(w) - \cos(w_s)}{\sin(w_s) - \frac{\pi w_s}{180}\cos w_s}\right) \tag{13}$$

With a and b constants given by

$$a = 0.409 + 0.516 \sin\left(w_s - \frac{60\pi}{180}\right) \tag{14}$$

$$b = 0.6609 - 0.4767 \sin\left(w_s - \frac{60\pi}{180}\right) \tag{15}$$

The hour angle (w) is adjusted by the Spencer Time equation [35] and the difference from each location longitude to the longitude of reference for Chile.

Then, based on [30] and Liu and Jordan [28] assumption that I_d/H_d is the same as I_0/H_0, where I_0 is the hourly extraterrestrial radiation, the hourly diffuse radiation I_d is obtained with the ratio of hourly diffuse to daily diffuse radiation r_d, which is defined as

$$r_d = \frac{I_d}{H_d} = \frac{\pi}{24}\left(\frac{\cos(w) - \cos(w_s)}{\sin(w_s) - (\pi w_s/180)\cos w_s}\right) \tag{16}$$

Finally, hourly beam radiation I_b is calculated by subtracting I_d from I.

4. Technology selection

The solar power plant considered in the model consists in three main circuits: the solar field, through which the heat transfer fluid (HTF) circulates; the power block (PB), where water and steam are circulated, equipped or not with an auxiliary boiler; and the thermal energy storage system (TES).

The solar field consists of a number of parabolic trough collector loops connected in parallel to each other [35]. Each loop consists of several solar collectors, which are made of highly reflective parabolic mirrors with receiver tubes mounted at the focal line of the parabolic surface. The solar collector total area varies according to each power plant capacity considered for the simulation [36]. The total CSP plant area is calculated according to a 1:4 proportion between the solar collector area and the total land area [21].

The HTF is distributed to the loops in the solar field by means of insulated pipes. A single-axis tracking mechanism allows the collectors to follow the sun from sunrise to sunset [37]. The sunlight reflected within the trough is focused along a line running the length of the trough. In order to collect this heat, a pipe is positioned along the length of the trough at its focus and a heat collection fluid is pumped through it [18]. The tube receiver is designed to be able to absorb most of the energy focused onto it and must be able to withstand the resultant high temperature. The solar array of a parabolic trough power plant consists of several parallel rows of parabolic reflectors. The heat collecting fluid, which is pumped through the pipes along the length of each solar trough, is typically synthetic oil, similar to engine oil, capable of operating at high temperature. During operation it is likely to reach between 300 °C and 400 °C [18].

After circulating through the receivers of the solar field, the oil is delivered to the power block, consisting of a heat exchanger train (preheaters, steam generators, superheaters, and reheaters), a steam turbine and electricity generator, a condenser, a wet cooling system (supplied from sea water pumped to the CSP plants site according to the volume that each power plant capacity requires [17]), and other auxiliary equipment [37]. The heat exchanger extracts the heat from the synthetic oil to raise the steam temperature in a separate sealed system. The steam is

then used in a Rankin cycle to drive a steam turbine generator to produce electricity. The heat collecting fluid is then cycled back through the solar collector field to get in more heat.

Considering solar power alternatives, the parabolic trough collector (PTC) power plant is seen as the most convenient for solar electricity generation due to its better performance than other alternatives and its status as the most developed technology [11,12]. The high quality and quantity of specific available data about PTC components and processes are the reasons why this technology was selected in the present study. One of the previous researches [4], in which this study is based in, selected the parabolic trough technology with a direct steam generation (DSG) process in order to decrease costs related with heat exchangers. Even though, we consider the traditional process using synthetic oil since the heat collection fluid, as described above, is a more mature and developed technology [18].

Since the solar radiation displays daily, seasonally and multi-annual variability, the configuration of the CSP plant counts with a storage system that consists of two tanks of molten salts sized for working 7 h at full load without solar irradiation [38]. At the design-point conditions, collectors receive the solar irradiation while they are cooled by means of the HTF. Thus, solar collectors produce the nominal mass flow of HTF at its nominal temperature. Because the solar field is oversized according to the solar multiple, part of the HTF mass flow is sent to the steam generator. The surplus mass flow is directed to the thermal storage system. In the charging mode, the molten salts are pumped from the cold tank, pass through a heat exchanger where they are heated and finally go to the hot tank at a slightly lower temperature than the nominal HTF temperature. When the solar irradiation is lower, i.e. at the sunset, production of HTF decreases. If the steam turbine is required to work at full load, the thermal storage system begins discharging the energy stored in the hot tank to the HTF. Therefore, part of the HTF by-passes the solar collectors and is warmed up by the molten salts. Molten salts are pumped from the hot tank; pass through the heat exchanger where they warm up the HTF and finally are discharged into the cold tank. Both flows, coming from the solar collectors and from the molten salt heat exchanger are mixed and then directed to the steam generator [18].

Also, in one of the plant arrangements, an additional gas-fired boiler will be incorporated to the system in order to supply backup heat during night, or stabilize steam properties to maintain a constant power output for cloudy days whenever the TES is not sufficient [39]. As the fossil fuel backup required for maintaining constant generation is function of the local conditions (radiation levels, clarity, temperature, and TES load level), the plant performance can significantly vary for different locations [4].

5. Levelized energy costs modeling

The core of this study is to compare the LECs given by different sizes of solar power plants placed in distinct locations of northern Chile. The LEC represents the generated electricity costs that include the initial capital, return of investment, and variable costs. It consists in the division of the total costs by the total energy produced. The result is referred as the levelized cost of energy, which is widely used to compare competing energy sources and is normally calculated using U.S. dollars. The formula for calculating LEC is the following:

$$\mathrm{LEC} = \frac{\mathrm{AIC}}{E_{annual}} \tag{17}$$

Table 2
Values of economics parameters used in the simulation.

Parameters	Value
Solar field and block of power investment [40]	6,059,461.70 US$/MW
Storage cost [17]	1,110,425.05 US$/MW
Backup investment cost [21]	134.960 US$/MW
Annual O&M cost [40]	70 US$/kW yr
Price for gas [14]	0.0164 US$/kWh
Discount rate (r)	10%
Life time of the plant (n)	25 yrs
Land rental costs [41]	305.3 US$/ha month
Annual costs for piping and pumping 100 MM m^3/yr [17]	Vertical: US$ 0.068/ m^3 × 100 m Horizontal: US$ 0.080/ m^3 × 100 Km

Table 3
Values of technical specifications used in the simulation.

Description	Value
Solar field efficiency [42]	0.492
Thermal energy storage efficiency [42]	0.996
Power block efficiency [42]	0.4
Pumping consumption [21]	10%

where E_{annual} is the annual electricity generation and AIC is the annualized cost, which is calculated as follows:

$$\mathrm{AIC} = \mathrm{TICVC}\frac{(1+r)^n r}{(1+r)^n - 1} \tag{18}$$

where r is the discount rate, n is the life time of the plant in years, and TICVC corresponds to the total investment costs and variable costs. In the total investments are considered the costs of the solar field, block of power, energy storage system, the gas-fired backup system, pipes and bombs for extracting sea water, and for cooling processes (annual costs for piping and pumping vary according to the distance from the plant location to the sea). Variable costs include annual operation and maintenance cost, price of natural gas used in the backup system, land rental cost and annual costs for pumping energy consumption, and the last one is specified in Table 3.

The variables used for the analysis are resumed in Table 2.

6. Simulation

The simulation algorithm is written and developed in MatLab commercial software. The inputs used for the analysis are: the estimation of daily radiation for each selected site and the investment and variable costs previously explained. As output, the simulation provides: the values of LEC, the proportion of solar energy from the total energy generated, and the capacity factor for every plant size and location. The power plant capacities analyzed vary between 5 and 200 MW, increasing 5 by 5 MW from the minimum value until the maximum value stipulated, which give us a number of 40 distinct power plants capacities being evaluated by the simulation model, for each location. To decide about the correct power capacity range to analyze, it was necessary to gather information of other plants currently in operation [21]. The optimal LEC in those plants was found to be around an installed capacity of 150 MW. Therefore, it was used a range between 5 MW and 200 MW for the present analysis.

The algorithm uses the geographical and meteorological data and the solar field area specifications to calculate the corresponding

solar time and angle of incidence of the solar radiation over a collector operating on sun-tracking mode. These results, together with calculations of the solar field efficiency, are used to obtain the useful thermal power energy delivered by the solar field. Depending of the thermal energy delivered, the decision of the plant's operating mode is determined (TES system and/or backup system operation). Consecutively, the corresponding thermal power is sent to the power block, which is calculated according to the correspondent specifications (energy storage efficiency and/or auxiliary boilers efficiency). These results pass through the efficiency specifications of the power block (PB) and then, are used to calculate the gross electric power generated, the plant's parasitic consumption and, finally, the net electricity production.

The code is programmed in such a way that the main function calculates, for every location and power plant capacity, the energy production of every hour of a single day. After a given hour is calculated, certain results (like the energy stored in the TES system) are saved as input for the calculation of the following hour. The finality is to calculate the final energy production of an entire year. Also, the algorithm separates the year into a summer and a winter seasons. This classification allows to differentiate the energy demand peak hours of these two periods. In summer, the peak hours are reached from 19:00 to 23:00. During winter, the peak hours occur from 18:00 to 23:00. The algorithm does not distinguish weekends and holidays, therefore the peak hours are applied for every day of the year according to its correspondent season.

An important aspect of the simulation model developed is that the minimum level of production of the PB can be set by the user [21]. In this work, the minimum load fraction (ML%) is defined at 30% of the nominal capacity of each plant size. This minimal operation level will determine the decision of when the energy storage or the auxiliary boiler will work and how much energy will be produced by them. When the radiation level is insufficient to produce at least at the minimal level stipulated, the thermal storage and/or the auxiliary power system are employed in parallel to produce the supplement of energy required to reach the ML%. However, in peak hours, the plant is considered to produce at nominal capacity, which means that is not necessary to the solar field to produce lower than the ML% to turn on the storage or backup supply.

The following steps describe the most important aspects of the algorithm used for calculating the annual energy production according to the ML%:

(i) The direct solar radiation is calculated in order to determine the energy flux received by the solar field.
(ii) If the thermal flux is higher than the required value to activate the plant at nominal capacity, the plant produces electricity just with solar energy. The excess energy is stored and the auxiliary system is off.
(iii) If it is not a peak hour and the energy production is not enough to reach 100% of the plant capacity, but it is higher than the minimum level to work at ML% of the capacity, the plant works with solar input from collectors. The stored energy does not change, and the auxiliary system is off.
(iv) If the collector steam production does not reach the minimum level of ML% in hour of regular consumption, there are two possibilities:
  (a) The energy storage is able to complement the collector field to reach the steam mass production necessary to activate the plant at the ML%. The plant works at ML% of its capacity and the energy in the storage tanks is consequently reduced.
  (b) The stored energy in the tanks is not sufficient to reach ML% of the nominal capacity of the plant. In this case, the auxiliary system is enabled to complement the production of the collector field and the tanks to activate the plant at a level of ML%.
(v) If it is a peak hour and the energy production is not enough to reach 100% of the plant capacity, a similar procedure as in (iv) will be performed in order to reach the full load capacity.

In addition to the previously described points, the algorithm searches and reserves the 10 consecutive days with lowest radiation levels in the year for performing maintenance. This procedure allows minimizing the costs of turning off the operation of the entire solar plant.

Also, a second simulation modality is performed, where no gas auxiliary system is used. For this to be done, the algorithm to produce energy is changed. The previous steps remain the same until step (iii), and step (iv) is changed: if the collector steam production and the energy storage do not reach the minimum level of ML%, then no energy is produced, the plant is off. Step (v) also changes in this second simulation, no peak hours are considered.

7. Results

For the 16 locations, the LECs evaluated for the first plant configuration (equipped with TES and back-up system) vary between 18.72 ¢US$/kWh and 21.85 ¢US$/kWh. The three best locations, according to the lowest LECs criteria, are Pica, Coya Sur, and Calama, as shown in Table 4. These LEC results are consistent with several references in the literature for solar thermal energy prices, such as [14,13,15].

Fig. 5 shows the results for hourly beam radiation (I_b) in October 22 for Pica. As shown, radiation peaks to levels of 3.68 MJ/m^2 h. However, this radiation levels are not the highest among all locations evaluated. This situation suggests that the consistency in time of the high levels of radiation allow these three locations to operate within a less expansive range, in opposite of other ones with higher radiation peaks, but no consistency in time of solar incidence levels.

Energy results in Table 4 show that Calama has the highest solar fraction of the annual electricity generation between the three locations, while Coya Sur uses the lowest fraction. Despite Calama

Table 4
Simulation results: LEC, solar production percentage and capacity factor percentage values of top three locations, Pica, Coya Sur, and Calama.

Parameter	Pica	Coya Sur	Calama
LEC [¢US$/kWh]	18.72	18.82	18.91
Solar production [%]	77.5	74.83	82.54
Capacity factor [%]	58.79	58.07	60.04

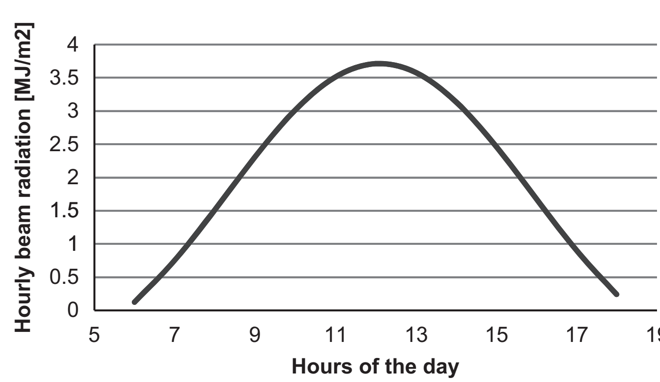


Fig. 5. Hourly radiation beam for Pica.

has a higher solar fraction than Pica and Coya Sur and a higher capacity factor than both others, its LEC is higher than the others. This is explained mainly by Calama's distance with the sea and altitude, what increases piping and pumping investment costs.

Results also show that a higher nominal power capacity is normally related to a lower LEC, as can be observed from a 200 MW plant in Pica, which have the lowest levelized costs. The same power capacity configuration was found for Coya Sur and Calama's best LEC values.

The results without auxiliary system show that the three best locations for solar energy in Chile are: Calama, with a LEC of 27.55 ¢US$/kWh and capacity factor of 39.57%; San Pedro de Atacama, with a LEC of 28.04 ¢US$/kWh and a capacity factor of 39.25%; and El Tatio, with a LEC of 28.29 ¢US$/kWh and a capacity factor of 41.85%. All three achieve these results with 200 MW of installed power capacity.

According to [4], the methodology used here for obtaining hourly beam radiations has a significant difference compared with another methodology that uses identical days with monthly mean radiation. This occurs because the second alternative has a significant loss in accuracy, which can impact on the usability of the collectors. Therefore, the results previously mentioned count with more accurate values of available radiation.

8. Conclusions

Considering global and local concerns and objectives regarding the environment and fossil fuels depletion, finding substitutes to conventional energy sources, such as solar energy has become a global issue.

It is known that the SING region, in northern Chile, will be highly affected by the increase in energy demand due to mining and industrial activity, that are very developed in this area. Solar resource in the Atacama Desert becomes, therefore, in an attractive alternative for energy generation in the north of the country. Considering this scenario, the present study presents an analysis of levelized energy cost (LEC) for different power capacities of CSP plants placed in distinct locations in northern Chile.

The results show that CSP plants can be implemented in Atacama Desert. For obtaining the optimal LEC, the recommended installed power capacity is 200 MW, where the location of Pica has the lowest LEC (18.72 ¢US$/kWh). Despite its large distance to the seacoast and radiations levels there are significantly high, allowing to obtain attractive levelized energy costs. LEC results are consistent with several references in the literature for solar thermal energy prices, such as [14,13,15].

The simulation of a plant functioning without auxiliary system shows that levelized energy costs are significantly higher than for plants that include this system, with differences of at least 9 ¢US$/kWh.

Due to shortage of both ground and surface water in Atacama Desert, sea water consumption was considered for feeding the cooling system in the simulations. It is noticed that this feature lead to significant cost surges in the analysis.

It is important to remark that the methodology used for estimating the available radiation has several limitations. First, the autoregressive nature of solar radiation was considered only indirectly, since the method is based on empirical correlations formulated by observing large data set. Therefore, they might include autoregressive effects. Second, the present work intends to model the conditions of northern Chile, where high clearness index results in a large number of clear days in any given month. As a result, the model is not valid for sites that display from moderate to large number of cloudy days in a given year. Finally, our procedure uses monthly averages in order to develop an artificial set of days for each month, and then uses daily totals to create an hourly database by means of a clear day model. The results could improve in accuracy if a database of hourly radiation empirically measured were currently available.

The authors are currently working in researches that analyze different methodologies to reduce costs of CSP plants in Chile, such as the trade of carbon emission reduction units.

Acknowledgements

The authors wish to acknowledge the Centre for Innovation in Energy of the University Adolfo Ibáñez for providing valuable assistance. Any remaining errors are those of the authors.

References

[1] Huepe C. Politica Energetica Nuevos Lineamientos: Transformando la crisis energética en una oportunidad. Comisión Nacional de Energía (CNE) 2008.
[2] Ortega A, Escobar R, Colle S, De Abreu SL. The state of solar energy resource assessment in Chile. Renewable Energy. 2010;35:2514–24.
[3] Escobar R, Larraín T. Net Energy Analysis for Concentrated Solar Power Plants in northern Chile. Renewable Energy 2011;41:123–33.
[4] Larraín T, Escobar R, Vergara J. Performance model to assist solar thermal power plant siting in northern Chile based on backup fuel consumption. Renewable Energy 2010;35:1632–43.
[5] D Daza Stindt, F. Martínez Andrade, Anteproyecto de factibilidad técnico-económica de utilización de la energía solar en Bayer de Chile SA, Universidad de Santiago de Chile. Facultad de Ingeniería, 1982.
[6] G. Osorio Vargas, Utilización de la radiación solar como fuente de energía en Chile, 〈http://hdl.handle.net/10533/53937〉, 1974.
[7] Frick G, Hirschmann J. Theory and experience with solar stills in Chile. Solar Energy 1973;14:405–13.
[8] Hirschmann JG. Records on solar radiation in Chile. Solar Energy 1973;14:129–38.
[9] Hirschmann JG. A solar energy pilot plant for northern Chile. Solar Energy 2003;5:37–43.
[10] Energy Balance, National Energy Commission (CNE), 2010.
[11] Stoddard L, Abiecunas J, O'Connell R. Economic, energy, and environmental benefits of concentrating solar power in California. National Renewable Energy Laboratory (NREL) 2006.
[12] Kaltschmitt M, Streicher W, Wiese A. Renewable energy: technology, economics, and environment. Springer Verlag; 2007.
[13] Reporte Especial Diciembre 2007 Abengoa Solar, 〈http://abengoa.com/htmlsites/boletines/es/diciembre2007ext/electrica.htm〉, (2007).
[14] World Energy Outlook, International Energy Agency (IEA), 2011.
[15] World Bank, Cost Reduction Study for Solar Thermal Power Plant, SolarPaces, 〈http://www.solarpaces.org/Library/docs/STPP%20Final%20Report2.pdf〉, (1999).
[16] Rovira A, Montes MJ, Valdes M, Martínez-Val JM. Energy management in solar thermal power plants with double thermal storage system and subdivided solar field. Applied Energy 2011;88:4055–66.
[17] Damerau K, Williges K, Patt AG, Gauché P. Costs of reducing water use of concentrating solar power to sustainable levels: scenarios for North Africa. Energy Policy 2011;39:4391–8.
[18] Poullikkas A. Economic analysis of power generation from parabolic trough solar thermal plants for the Mediterranean region—a case study for the island of Cyprus. Renewable and Sustainable Energy Reviews 2009;13: 2474–84.
[19] Viebahn P, Lechon Y, Trieb F. The potential role of concentrated solar power (CSP) in Africa and Europe—a dynamic assessment of technology development, cost development and life cycle inventories until 2050. Energy Policy 2010;39:4420–30.
[20] Izquierdo S, Montañés C, Dopazo C, Fueyo N. Analysis of CSP plants for the definition of energy policies: the influence on electricity cost of solar multiples, capacity factors and energy storage. Energy Policy 2010;38: 6215–21.
[21] Cabello J, Cejudo J, Luque M, Ruiz F, Deb K, Tewari R. Optimization of the size of a solar thermal electricity plant by means of genetic algorithms. Renewable Energy 2011;36:3146–53.
[22] Kreith F, Goswami DY. Principles of sustainable and renewable energy. 1st ed.CRC Press; 2011.
[23] Duffie J, Beckmann W. Solar engineering of thermal processes, Wiley. 3rd ed. USA: John Wiley and Sons; 2006.
[24] Sarmiento P. Energía solar: Aplicaciones e ingeniería, Ediciones Universitarias de la Universidad Católica Valparaíso. Valparaíso 1995.
[25] A Ortega, R Escobar, S. Colle, Solar Energy Resource Assessment for Chile, en: International Conference on Energy Sustainability, Jacksonville, USA, 2008.
[26] Mainguet M. Aridity: droughts and human development. Berlin: Springer; 1999.

[27] CNE/PNUD/UTFSM, Irradiancia Solar en Territorios de la República de Chile, Proyecto CHI/00/G32, 2008.
[28] Liu BYH, Jordan RC. The interrelationship and characteristic distribution of direct, diffuse and total solar radiation. Solar Energy 1960;4:1–19.
[29] Bendt P, Collares-Pereira M, Rabl A. The frequency distribution of daily insolation values. Solar Energy 1981;27:1–5.
[30] Aguiar R, Collares-Pereira M. TAG: a time-dependent, autoregressive, Gaussian model for generating synthetic hourly radiation. Solar Energy 1992;49:167–74.
[31] Stuart R, Hollands K. A probability density function for the beam transmittance. Solar energy 1988;40:463–7.
[32] Knight K, Klein S, Duffie J. A methodology for the synthesis of hourly weather data. Solar Energy 1991;46:109–20.
[33] Santos J, Pinazo J. Methodology for generating daily clearness index values Kt starting from the monthly average daily value. Determining the daily sequence using stochastic models. Renewable energy 2003;28:1523–44.
[34] Cooper P. The absorption of radiation in solar stills. Solar Energy 1969;12: 333–46.
[35] 〈http://www.renewables-made-in-germany.com/en〉; 2011[accessed 19/09/2011].
[36] Fernández-García A, Zarza E, Valenzuela L, Pérez M. Parabolic-trough solar collectors and their applications. Renewable and Sustainable Energy Reviews 2010;14:1695–721.
[37] Llorente García I, Álvarez JL, Blanco D. Performance model for parabolic trough solar thermal power plants with thermal storage: comparison to operating plant data. Solar Energy 2011;85:2443–60.
[38] Herrmann U, Kelly B, Price H. Two-tank molten salt storage for parabolic trough solar power plants. Energy 2004;29:883–93.
[39] Müller-Steinhagen H, Trieb F. Concentrating solar power, quarterly of the royal academy of engineering. Ingenia 2004.
[40] C. Turchi, M. Mehos, C. Ho, G. Kolb, Current and future costs for parabolic trough and power tower systems in the US market, (2010).
[41] Cuentas Públicas Nacionales, Ministerio de Bienes Nacionales, 〈http://www.bienesnacionales.cl/planificacion-y-presupuesto/cuentas-publicas/〉, 2009.
[42] Sargent and Lundy Consulting Group. Assessment of parabolic trough and power tower solar technology cost and performance forecasts. National Renewable Energy Laboratory (NREL) 2003.